Acta Crystallographica Section B
Structural Science
ISSN 0108-7681

Isobaric and isochoric freezing of CH_2BrCl and isostructural relations between CH_2Cl_2, CH_2Br_2 and CH_2BrCl

Marcin Podsiadło and Andrzej Katrusiak*

Faculty of Chemistry, Adam Mickiewicz University, Grunwaldzka 6, 60-780 Poznań, Poland

Correspondence e-mail: katran@amu.edu.pl

Received 17 August 2007
Accepted 12 September 2007

Bromochloromethane, CH_2BrCl, has been temperature-frozen and *in situ* pressure-frozen and the structure determined by X-ray diffraction at low temperatures of 170 and 100 K at ambient pressure (0.10 MPa), and at high pressures of 1.04 and 1.72 GPa at room temperature (295 K). CH_2BrCl exhibits a remarkable polymorphism: at low temperature it crystallizes in the monoclinic space group $C2/c$ (phase I), isostructural to the crystals of CH_2Br_2. The pressure-frozen crystal of CH_2BrCl is orthorhombic, space group *Pbcn*, and is isostructural to the crystal of CH_2Cl_2. In both phases I and II the Br and Cl atoms are substitutionally disordered. The freezing temperatures and pressures of simple dihalomethanes have been correlated to their molecular weight and halogen···halogen distances. Calculated electrostatic potential surfaces have been related to the different crystal packing of dihalomethanes investigated.

1. Introduction

Methanes are the simplest organic compounds and their structures are of fundamental interest. Small bulky and weakly interacting methane molecules are model structures for the studies of cohesion forces between organic molecules and of their aggregation. Structures of halogenated methanes are dominated by halogen···halogen contacts, described as donor–acceptor interactions, charge-transfer interactions, 'secondary' interactions or as the interactions between the highest-occupied molecular orbitals and the lowest-unoccupied molecular orbitals (Rosenfield *et al.*, 1977; Guru Row & Parthasarathy, 1981; Ramasubbu *et al.*, 1986; Desiraju & Parthasarathy, 1989). In the absence of hydrogen bonds, and when the close-packing effect is less important for small than for large molecules, the specific patterns of molecules in the crystal structures of halogenated compounds are mainly governed by the halogen···halogen interactions. These interactions can also considerably modify the properties of materials (Bosch & Barnes, 2002; Metrangolo & Resnati, 2001; Zaman *et al.*, 2004). Meanwhile, there is still no unanimous opinion about the role of halogen···halogen interactions in molecular aggregation. While there are reports on molecular attraction to the halogen atoms (Zordan & Brammer, 2004; Awwadi *et al.*, 2006), there are also arguments for the repulsion of the halogens, *e.g.* chlorophobic interactions (Grineva & Zorkii, 2000, 2001, 2002; Boese *et al.*, 2001; Grineva *et al.*, 2007). Also the role of different types of intermolecular interactions in the formation of hydrogen-bonded aggregates is still not fully understood. This applies to a large group of inorganic and natural compounds. Although high-pressure methods are often used to study molecular association in biologically important compounds and pharmaceutical drugs

(*e.g.* Boldyreva, 2003; Boldyreva *et al.*, 1998, 2005), the structural studies of compounds without hydrogen bonds can elucidate the difference between molecular arrangements using the close-packing principle (Kitaigorodskii, 1973) and the weak intermolecular interactions, *e.g.* of the halogen-···halogen type.

Most recently, we have studied a series of dihalomethanes, CH_2X_2, where X = Br, Cl and I. Although their molecules have very similar shapes, they crystallize in different space groups. The temperature- and pressure-frozen CH_2Cl_2 crystals are orthorhombic, with space group *Pbcn* (Kawaguchi, Tanaka, Takeuchi & Watanabé, 1973; Podsiadło *et al.*, 2005), while CH_2Br_2 forms a monoclinic structure, with space group *C*2/*c* (Kawaguchi, Wakabayashi, Matsumoto, Takeuchi & Watanabé, 1973; Podsiadło *et al.*, 2006). Temperature-frozen CH_2I_2 crystallizes either in monoclinic *C*2/*c* symmetric metastable phase I, or in orthorhombic and polar *Fmm*2 symmetric stable phase II (Kawaguchi, Wakabayashi, Matsumoto, Takeuchi & Watanabé, 1973; Prystupa *et al.*, 1989), whereas only phase II was obtained by pressure freezing (Podsiadło *et al.*, 2006). Presently we complete our studies of dihalomethanes with CH_2BrCl phases, the first dihalomethane in this series of structures with different halogen atoms. By undertaking this investigation we hoped to reveal the preference of homo- or heterohalogen intermolecular contacts between the Br and Cl atoms. Simple ionic salts with Cl^- and Br^- anions are textbook examples of solid solutions (Kitaigorodskii, 1983), thus it was also intended to investigate the preference of CH_2BrCl to crystallize with the molecules orientationally disordered, and the same sites half-occupied by Cl and Br atoms.

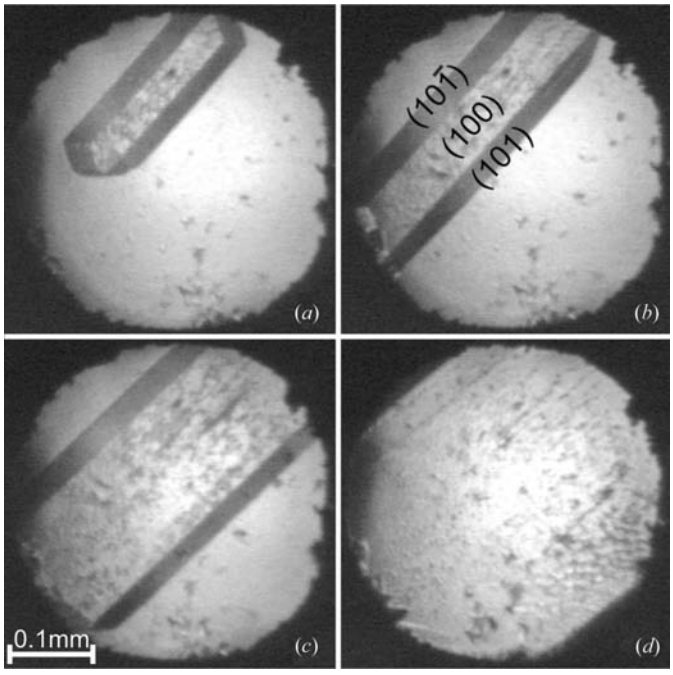

Figure 1
The phase II CH_2BrCl single-crystal growth stages from the grain (*a*) at 430 K to the crystal-filling whole volume of the high-pressure chamber at 1.72 GPa/295 K (*d*). The Miller indices of the crystal faces have been indicated in (*b*). The ruby chip for pressure calibration (Barnett *et al.*, 1973; Piermarini *et al.*, 1975) is at the bottom-left (at 8 o'clock) edge of the chamber.

2. Experimental

Bromochloromethane (m.p. 185 K), analytical grade from Polskie Odczynniki Chemiczne, has been used without further purification and loaded onto a four-pin diamond–anvil cell (DAC). The gasket was made of 0.1 mm thick carbon-steel foil with the spark-eroded and a pre-indented hole. At 1.04 GPa polycrystalline CH_2BrCl filled the whole volume of the high-pressure chamber, which was 0.31 mm in diameter and 0.05 mm in height. The pressure was calibrated using the ruby-fluorescence method (Barnett *et al.*, 1973; Piermarini *et al.*, 1975), with a BETSA PRL spectrometer (accuracy 50 MPa). All the crystal grains except one seed were melted using the hot-air gun and then the single crystal was grown by cooling the DAC. This single crystal of CH_2BrCl entirely filled the volume of the high-pressure chamber at room temperature. Another gasket, with the pressure chamber 0.38 mm in diameter and 0.08 mm in height, was used for the experiment at 1.72 GPa. The growth stages of CH_2BrCl single crystals in the high-pressure chamber are shown in Fig. 1.

The isobaric crystallization of CH_2BrCl was carried out in a sealed glass capillary with an internal diameter of 0.3 mm and a wall 0.01 mm thick. The liquid sample which filled *ca* 1 mm of the capillary was cooled in a nitrogen gas stream from an Oxford Cryosystems attachment. Setting the temperature of the gas stream to 150 K yielded a polycrystalline material, which was heated to *ca* 180 K. Growth of the single crystal was achieved by cycling (increasing and lowering repeatedly about 50 times) the temperature at a rate of 1 K min^{-1}, within the range 180–181 K which is close to the melting point, gradually eliminating all the crystal seeds but one, which eventually grew from all the sample contained in the capillary (see the crystal size in Table 1). The first X-ray intensity data were collected at 170 K, and the second at 100 K.

The low-temperature/ambient-pressure and room-temperature/high-pressure diffraction data were collected on a KM-4 CCD diffractometer, operating with graphite-monochromated Mo $K\alpha$ radiation. At 170 and 100 K the reflections were measured using the ω-scan techniques with $\Delta\omega = 0.8^\circ$ and 20 s exposure time. The DAC in high-pressure experiments was centred by the gasket-shadow method (Budzianowski & Katrusiak, 2004). The images were recorded using the ω-scan technique, with 0.85° ω frames and 30 s exposures at 1.04 GPa, and 0.7° ω frames and 30 s exposures at 1.72 GPa (Budzianowski & Katrusiak, 2004).

The *CrysAlis* programs (Oxford Diffraction, 2004) have been used for data collection, determination of the crystal-orientation matrices, initial data reductions and *Lp* corrections. In the case of high-pressure measurements, the reflection intensities have been corrected for the effects of the absorption of X-rays by the DAC, shadowing the beams by the gasket edges, and the absorption of the sample crystal itself (Katrusiak, 2003, 2004). The symmetry of the crystals has been unequivocally determined from systematic absences. The

Table 1
Crystal data and details of the refinements of CH_2BrCl low-temperature phase I at 0.10 MPa/170 K and 0.10 MPa/100 K, and high-pressure phase II at 1.04 GPa/295 K and 1.72 GPa/295 K.

	170 K, 0.10 MPa	100 K, 0.10 MPa	295 K, 1.04 GPa	295 K, 1.72 GPa
Crystal data				
Chemical formula	CH_2BrCl	CH_2BrCl	CH_2BrCl	CH_2BrCl
M_r	129.39	129.39	129.39	129.39
Cell setting, space group	Monoclinic, *C*2/*c*	Monoclinic, *C*2/*c*	Orthorhombic, *Pbcn*	Orthorhombic, *Pbcn*
Temperature (K)	170 (1)	100 (1)	295 (2)	295 (2)
a, *b*, *c* (Å)	11.959 (2), 4.4531 (9), 14.873 (3)	11.874 (2), 4.4224 (9), 14.582 (3)	4.1126 (8), 8.0685 (16), 9.755 (2)	3.9929 (8), 7.9351 (16), 9.6808 (19)
β (°)	112.96 (3)	112.04 (3)	90.00	90.00
V (Å^3)	729.3 (3)	709.8 (2)	323.69 (11)	306.73 (11)
Z	8	8	4	4
D_x (Mg m^{-3})	2.357	2.422	2.655	2.802
Radiation type	Mo $K\alpha$	Mo $K\alpha$	Mo $K\alpha$	Mo $K\alpha$
μ (mm^{-1})	11.73	12.05	13.21	13.94
Crystal form, colour	Irregular, colourless	Irregular, colourless	Cylinder, colourless	Cylinder, colourless
Crystal size (mm)	0.12 × 0.12 × 0.10	0.12 × 0.12 × 0.10	0.31 × 0.31 × 0.05	0.38 × 0.38 × 0.08
Data collection				
Diffractometer	KM-4 CCD	KM-4 CCD	KM-4 CCD	KM-4 CCD
Data collection method	ω scans	ω scans	φ and ω scans	φ and ω scans
Absorption correction	Multi-scan (based on symmetry-related measurements)	Multi-scan (based on symmetry-related measurements)	Numerical	Numerical
T_{min}	0.22	0.22	0.18	0.13
T_{max}	0.32	0.32	0.42	0.31
No. of measured, independent and observed reflections	2422, 909, 643	3122, 923, 784	2144, 160, 126	2283, 295, 271
Criterion for observed reflections	$I > 2\sigma(I)$	$I > 2\sigma(I)$	$I > 2\sigma(I)$	$I > 2\sigma(I)$
R_{int}	0.109	0.078	0.083	0.057
θ_{max} (°)	29.1	29.7	29.9	29.6
Refinement				
Refinement on	F^2	F^2	F^2	F^2
$R[F^2 > 2\sigma(F^2)]$, $wR(F^2)$, S	0.066, 0.172, 1.15	0.051, 0.128, 1.12	0.030, 0.058, 1.05	0.029, 0.065, 1.20
No. of reflections	909	923	160	295
No. of parameters	36	36	25	25
H-atom treatment	Mixture of independent and constrained refinement	Mixture of independent and constrained refinement	Mixture of independent and constrained refinement	Mixture of independent and constrained refinement
Weighting scheme	$w = 1/[\sigma^2(F_o^2) + (0.0777P)^2]$, where $P = (F_o^2 + 2F_c^2)/3$	$w = 1/[\sigma^2(F_o^2) + (0.0553P)^2 + 4.5134P]$, where $P = (F_o^2 + 2F_c^2)/3$	$w = 1/[\sigma^2(F_o^2) + (0.0301P)^2]$, where $P = (F_o^2 + 2F_c^2)/3$	$w = 1/[\sigma^2(F_o^2) + (0.031P)^2 + 0.0922P]$, where $P = (F_o^2 + 2F_c^2)/3$
$(\Delta/\sigma)_{max}$	0.009	< 0.0001	< 0.0001	< 0.0001
$\Delta\rho_{max}$, $\Delta\rho_{min}$ (e Å^{-3})	0.83, −0.65	1.51, −0.72	0.18, −0.23	0.35, −0.34
DAC transmission min/max	–	–	0.61/0.95	0.62/0.94
Gasket shadowing min/max	–	–	0.81/0.99	0.81/0.99
Sample transmission	0.22/0.32	0.22/0.32	0.36/0.45	0.25/0.33
Extinction method	*SHELXL*	*SHELXL*	*SHELXL*	*SHELXL*
Extinction coefficient	0.036 (4)	0.0023 (9)	0.014 (5)	0.005 (2)

Computer programs used: *CrysAlisCCD* and *CrysAlisRED* (Oxford Diffraction, 2004), *REDSHABS* (Katrusiak, 2003), *SHELXS*97 (Sheldrick, 1997*a*), *SHELXL*97 (Sheldrick, 1997*b*), *X-seed 2.0* (Barbour, 2001).

CH_2BrCl structures were solved by direct methods using *SHELXS*97 (Sheldrick, 1997*a*), and refined with anisotropic displacement parameters for non-H atoms by *SHELXL*97 (Sheldrick, 1997*b*).

In the low-temperature phase (space group *C*2/*c* and $Z = 8$) the molecules are located in general positions, but there was no distinction in the solved model between the Cl and Br sites. Attempts were made to refine the model with ordered CH_2BrCl molecules, but the best refinement was obtained for disordered Br and Cl atoms at the same sites with 0.5 occupancies. For each site one common set of anisotropic displacement parameters for Br and Cl atoms was refined as free variables. The H atoms were located from molecular geometry with the C—H bond length restrained to 0.97 Å (Sheldrick, 1997*a*,*b*) and their isotropic displacement parameters set at 1.2 times U_{eq} for the C atom.

The high-pressure crystal symmetry of space group *Pbcn* and $Z = 4$ implied that the molecules are located on twofold axes and that the Br and Cl atoms are disordered. Attempts were also made to refine several lower-symmetry models of the structure, but only the stable refinement was obtained for the *Pbcn* space group and the Br and Cl atoms at the same site

Table 2
Molecular geometry and intermolecular distances (Å) and angles (°) in CH_2BrCl phase I compared with the temperature- and pressure-frozen CH_2Br_2 structures.

Angle ω is the inclination of the molecular Br1—C1—Br2 plane to the crystallographic plane (001).

CH_2BrCl at	0.10 MPa/170 K[a]	0.10 MPa/100 K[a]	CH_2Br_2 at	0.10 MPa/183 K[b]	0.10 MPa/15 K†	0.61 GPa/295 K[c]
C1—H1	0.97	0.97	C1—H1	1.070	1.051 (7)	0.97
C1—H2	0.97	0.97	C1—H2	1.071	1.077 (7)	0.97
C1—Br1(Cl1)	1.837 (6)	1.863 (4)	C1—Br1	1.922	1.928 (5)	1.888 (15)
C1—Br2(Cl2)	1.871 (6)	1.870 (4)	C1—Br2	1.901	1.954 (5)	1.961 (16)
Br1(Cl1)···Br2(Cl2)	3.064 (1)	3.070 (1)	Br1···Br2 (Å)	3.165	3.188 (4)	3.201 (3)
∠Br1(Cl1)—C1—Br2(Cl2)	111.4 (1)	110.7 (1)	∠Br1—C1—Br2	112	110.4 (2)	112.5 (7)
∠H1—C1—H2	107.0 (3)	111.5 (2)	∠H1—C1—H2	109.5	116.9 (6)	107.84
Intermolecular contacts			Intermolecular contacts			
Br1(Cl1)···Br2(Cl2)^{i}	3.608 (1)	3.568 (1)	Br1···Br2^{i}	3.623	3.551	3.490 (3)
Br1(Cl1)···Br2(Cl2)^{ii}	3.734 (1)	3.677 (1)	Br1···Br2^{ii}	3.788	3.621	3.623 (3)
Br2(Cl2)···Br2(Cl2)^{iii}	3.836 (2)	3.786 (2)	Br2···Br2^{iii} (Å)	3.801	3.784	3.868 (12)
H2···Br1(Cl1)^{i}	3.006 (1)	3.010 (1)	H2···Br1^{iv}	3.032	3.066	3.036
∠ω	19.77 (12)	17.93 (8)	∠ω	11.59	13.33	1.46 (13)
∠C1—Br1(Cl1)···Br2(Cl2)^{i}	169.0 (1)	170.5 (1)	∠C1—Br1···Br2^{i}	173.15	174.89	179.3 (12)
∠C1—Br2(Cl2)···Br1(Cl1)^{v}	113.1 (1)	111.4 (1)	∠C1—Br2···Br1^{v}	113.32	109.33	112.7 (4)

References: (*a*) this work; (*b*) Kawaguchi, Wakabayashi, Matsumoto, Takeuchi & Watanabé (1973); (*c*) Podsiadło *et al.* (2006). Symmetry codes: (i) $-\frac{1}{2}+x,\frac{1}{2}+y,z$; (ii) $-\frac{1}{2}+x,-\frac{1}{2}+y,z$; (iii) $\frac{1}{2}-x,\frac{3}{2}-y,-z$; (iii) $x,y-1,z$; (iv) $\frac{1}{2}-x,-\frac{1}{2}+y,\frac{1}{2}-z$; (v) $\frac{1}{2}+x,-\frac{1}{2}+y,z$. † Low-temperature structure of CD_2Br_2 by neutron powder diffraction according to Prystupa *et al.* (1989).

with 0.5 occupancy. The anisotropic displacement parameters of Br and Cl were refined independently, because doing so significantly improved the model and reduced the *R* factors compared with the refinement with common U^{ij}s. The H atom was located from molecular geometry with the C—H bond length constrained to 0.97 Å (Sheldrick, 1997*a*,*b*) and its isotropic displacement parameters set at 1.2 times U_{eq} for the C atom. Selected details of the temperature- and pressure-frozen structure refinements and crystal data are listed in Table 1. The final atomic parameters have been deposited.[1]

The *GAUSSIAN*03 program suite and a PC were used to calculate the electrostatic potential on the molecular surface of dihalomethanes (Frisch *et al.*, 2003). The DFT calculations were carried out at the B3LYP/3-21G** level of theory. The electrostatic potential was mapped onto a molecular surface, defined as the 0.001 a.u. electron-density envelope (Bader *et al.*, 1987).

The compressibility measurements of dihalomethane compounds have been performed on cylinder-and-piston apparatus, described previously by Baranowski & Moroz (1982), with an initial volume of 9.8 ml.

The crystals obtained in two high-pressure crystallizations were oriented differently with respect to the DAC axis: at 1.04 GPa the crystal had its [001] axis parallel to the DAC axis, and at 1.72 GPa the [100] crystal direction was parallel to the DAC axis. The observation of various crystal orientations is consistent with some of our previous experiments, but contrary to those by Weir *et al.* (1969) who observed that the pressure-frozen crystals did not change their orientation with respect to the diamond culets.

[1] Supplementary data for this paper are available from the IUCr electronic archives (Reference: AV5094). Services for accessing these data are described at the back of the journal.

3. Discussion

3.1. CH_2BrCl phase I

The low-temperature *C*2/*c* crystal structure of the CH_2BrCl phase I is isostructural with that of the CH_2Br_2 crystals

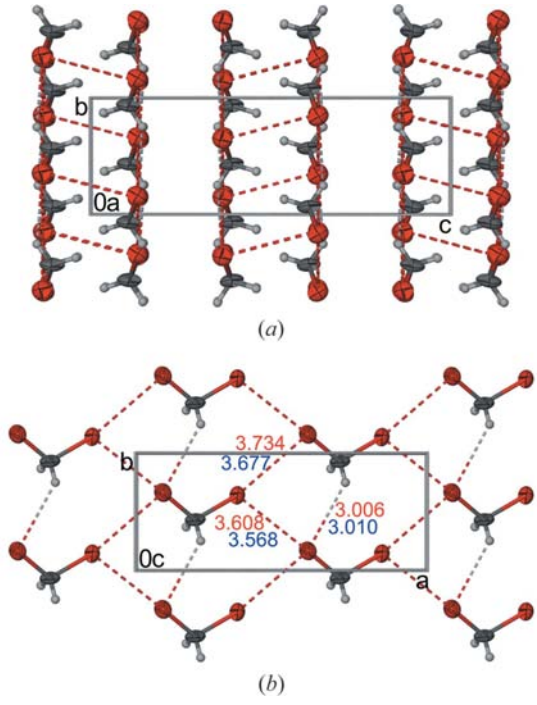

Figure 2
The molecular arrangement in CH_2BrCl phase I: (*a*) layers of molecules perpendicular to the crystallographic [001] direction; (*b*) projection of the layer shown in (*a*) on the *xy* plane. The shortest halogen···halogen and hydrogen···halogen intermolecular interactions are indicated with dashed lines (distances in red for 170 K and in blue for 100 K). The displacement ellipsoids are shown at the 50% probability level.

obtained by pressure- and temperature-freezing, and with CH_2I_2 phase I (Kawaguchi, Wakabayashi, Matsumoto, Takeuchi & Watanabé, 1973; Prystupa *et al.*, 1989; Podsiadło *et al.*, 2006). In phase I the CH_2BrCl molecules lie in general positions, but in contrast to the pressure-frozen CH_2Br_2 structure they are significantly inclined towards the crystallographic planes (001) at z = 1/8, 3/8 *etc.* (see Fig. 2). In the pressure-frozen CH_2Br_2 the inclination (ω angle) of the molecular plane, defined by atoms Br1—C—Br2, to the (001) plane is 1.46 (13)°, while in the CH_2BrCl phase I determined at 100 K the angle is 17.93 (8)°.

Inter- and intramolecular distances and angles in the CH_2BrCl phase I are compared with the CH_2Br_2 structures in Table 2. It is characteristic that all intramolecular distances involving disordered Br/Cl in CH_2BrCl are shorter than in CH_2Br_2, whereas no systematic differences are observed in intermolecular distances. The CH_2BrCl phase I can be considered as built of layers running along the shortest intermolecular halogen···halogen contacts (see Fig. 2). In phase I CH_2BrCl molecules in one layer have the same orientation (with the dipole moment almost parallel to [010]), and this molecular orientation is common for two neighbouring layers at z = 1/8 and 3/8 (Fig. 2*a*). The next two layers, at z = 5/8 and 7/8, are related to the first layer by inversion centres, and thus the molecular orientation is opposite.

3.2. CH_2BrCl phase II

The pressure-frozen CH_2BrCl II phase and CH_2Cl_2 are isostructural (Podsiadło *et al.*, 2005). Both compounds crystallize in the space group *Pbcn* with molecules located on one set of crystallographic twofold axes. The compressibility of the CH_2BrCl crystal is anisotropic. The linear coefficients calculated between 1.04 and 1.72 GPa are: $\beta_a = -0.043$, $\beta_b = -0.024$, $\beta_c = -0.011$ GPa^{-1}. These values are consistent with the data of the pressure-frozen CH_2Cl_2 (Podsiadło *et al.*, 2005), but CH_2BrCl along **a** and **b** is less compressed. The anisotropic compressibility of the crystal reflects the molecular arrangement and interactions. The shortest halogen···halogen contacts are formed between molecules arranged in corrugated sheets perpendicular to [010], as illustrated in Fig. 3(*a*), and in this respect the CH_2BrCl structure can be considered as built of layers. Each halogen atom forms two short halogen···halogen contacts, shorter than the sum of the van der Waals radii (Batsanov, 2001; Kitaigorodskii, 1973; Nyburg & Faerman, 1985), to its neighbours (see Fig. 3*b*). There are no short halogen···halogen and hydrogen···halogen interactions between the layers perpendicular to [010], while such interlayer contacts were present in its dichloro analogue. The orientation of the CH_2BrCl molecule can be conveniently described by the angle φ (see Fig. 3*b*) between the [001] axis and the projection of the C–halogen bond on the xz plane (Kawaguchi, Tanaka, Takeuchi & Watanabé, 1973). As in CH_2Cl_2, in the CH_2BrCl structure the φ angle (see Table 3) also decreases with pressure, but this dependence is much weaker ($\partial\varphi/\partial p$ = −0.03 (2)° GPa^{-1} in CH_2Cl_2 *versus* −0.01 (2)° GPa^{-1} in CH_2BrCl). The molecular dimensions and angles in pressure-frozen CH_2BrCl and CH_2Cl_2 are compared in Table 3. All the molecular dimensions and intermolecular contacts involving disordered Br/Cl sites in CH_2BrCl are systematically longer than the corresponding ones involving Cl in CH_2Cl_2.

According to Nyburg & Faerman (1985) the major radii of Br and Cl atoms are 1.84 and 1.78 Å respectively, while the minor radii of these atoms are 1.54 (Br) and 1.58 Å (Cl). Calculated sums of the anisotropic van der Waals Br and Cl radii in the CH_2BrCl phase II structure are presented in Table 4. Relatively small differences between the elliptical shapes of

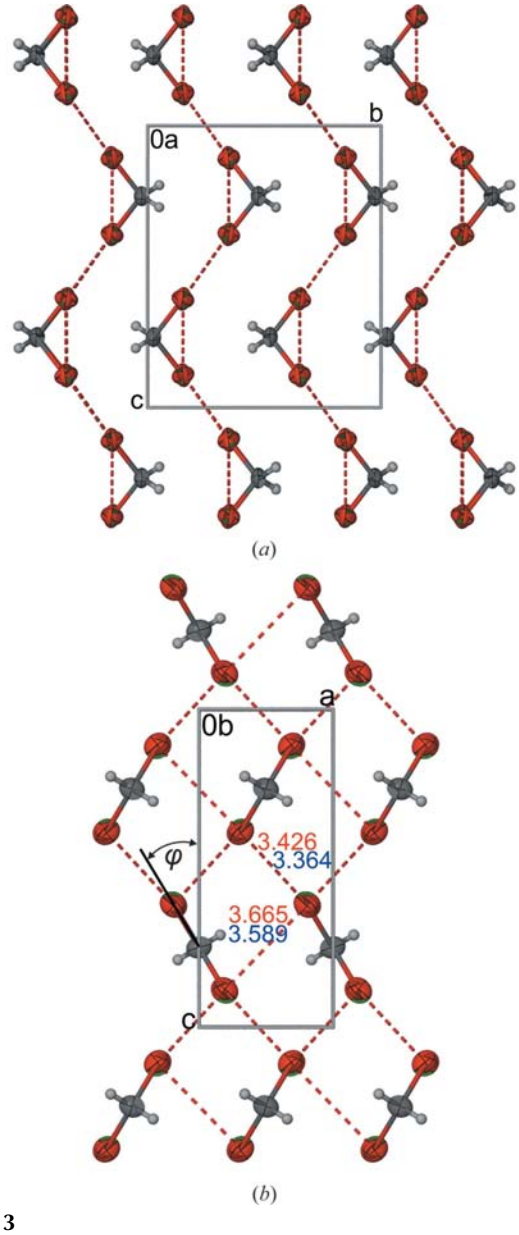

Figure 3
The molecular arrangement in CH_2BrCl phase II: (*a*) layers of molecules perpendicular to the crystallographic [010] direction; (*b*) projection of the layer shown in (*a*) on the xz plane. The shortest halogen···halogen intermolecular interactions are indicated with dashed lines (distances in red for 1.04 GPa and in blue for 1.72 GPa). The displacement ellipsoids are shown at the 50% probability level. The Br and Cl atoms, refined at the same site with the 0.5 occupancy, are superimposed.

Table 3
The molecular geometry and intermolecular distances (Å) and angles (°) in pressure-frozen CH_2BrCl and CH_2Cl_2 structures.

CH_2BrCl	1.04 GPa/295 K[a]	1.72 GPa/295 K[a]	CH_2Cl_2	1.33 GPa/295 K[b]	1.63 GPa/295 K[b]
C1—H1	0.9700 (1)	0.9700 (1)	C1—H1	1.01 (9)	1.13 (12)
C1—Cl1	1.844 (2)	1.853 (1)	C1—Cl1	1.765 (4)	1.769 (5)
C1—Br1	1.844 (2)	1.853 (1)			
Cl1···Br1	3.073 (3)	3.071 (1)	Cl1···Cl1*A*	2.919 (5)	2.922 (7)
∠Cl1—C1—Br1	112.91 (8)	111.94 (5)	∠Cl1—C1—Cl1*A*	111.6 (3)	111.4 (4)
Intermolecular contacts			Intermolecular contacts		
Cl1···Br1^{i}	3.426 (3)	3.364 (1)	Cl1···Cl1^{ii}	3.360 (3)	3.324 (5)
Cl1···Br1^{iii}	3.665 (3)	3.589 (1)	Cl1···Cl1^{iii}	3.522 (4)	3.496 (6)
Cl1···Br1^{iv}	3.672 (3)	3.602 (1)	Cl1···Cl1^{v}	3.534 (3)	3.498 (5)
Br1···H1^{vi}	3.012 (7)	2.954 (6)	Cl1···H1^{vii}	2.77 (12)	2.86 (14)
∠φ	30.76 (4)	30.63 (2)	∠φ	31.07 (7)	30.76 (9)
∠C1—Cl1···Br1^{i}	117.84 (2)	118.58 (2)	∠C1—Cl1···Cl1^{ii}	118.31 (7)	118.77 (7)
∠C1—Cl1···Br1^{viii}	168.17 (5)	168.40 (2)	∠C1—Cl1···Cl1^{ix}	168.72 (11)	168.64 (12)
∠C1—Cl1···Br1^{iii}	77.26 (7)	76.15 (2)	∠C1—Cl1···Cl1^{iii}	78.34 (9)	77.54 (14)

References: (*a*) this work; (*b*) Podsiadło *et al.* (2005). Symmetry codes: (i) $-\frac{1}{2}+x,\frac{3}{2}-y,1-z$; (ii) $-\frac{1}{2}+x,\frac{1}{2}-y,-z$; (iii) $1-x,y,\frac{1}{2}-z$; (iv) $-x,2-y,1-z$; (v) $-x,-y,-z$; (vi) $\frac{1}{2}+x,-\frac{1}{2}+y,\frac{1}{2}-z$; (vii) $\frac{1}{2}-x,\frac{1}{2}+y,z$; (viii) $\frac{1}{2}+x,\frac{3}{2}-y,1-z$; (ix) $\frac{1}{2}+x,\frac{1}{2}-y,-z$.

Table 4
Shortest intermolecular halogen···halogen distances (Å).

These distances are calculated by assuming the elliptical shape of the van der Waals spheres, and by applying the formula $r=(R_s^2\cos^2\theta+R_l^2\sin^2\theta)^{1/2}$, where θ is the C–halogen···halogen angle observed in the crystal structure of bromochloromethane phase II at 1.04 and 1.72 GPa and dichloromethane at 1.33 and 1.63 GPa, and R_s and R_l are the minor and major halogen radii (Nyburg & Faerman, 1985).

	1.04 GPa	1.72 GPa		1.33 GPa	1.63 GPa
CH_2BrCl	Calculated sums of van der Waals radii (Å)		CH_2Cl_2[a]	Calculated sums of van der Waals radii (Å)	
Cl1···Cl2	3.327	3.325	Cl1···Cl2	3.325	3.324
Cl1···Br2	3.292	3.290			
Br1···Cl2	3.368	3.364			
Br1···Br2	3.333	3.329			
	Distances observed in CH_2BrCl phase II			Distances observed in pressure-frozen CH_2Cl_2	
Br1(Cl1)···Br2(Cl2)	3.426	3.364	Cl1···Cl2	3.360	3.324

References: (*a*) Podsiadło *et al.* (2005).

the Br and Cl atoms can permit disorder in the crystal structure. Calculated sums of the van der Waals radii of Br and Cl atoms (Nyburg & Faerman, 1985) are exactly the same as those observed in the CH_2Cl_2 and CH_2BrCl phase II structures in the experiments performed at 1.63 and 1.72 GPa, respectively (see Table 4).

The lattice parameters, crystal morphology, shortest intermolecular halogen···halogen distances and compressibility of the bromochloromethane phase II and dichloromethane crystals are similar. The shortest lattice parameter *a* correlates with the crystal growth rates in this manner, so the crystal grain grew fastest along [010] across the chamber (see Fig. 1).

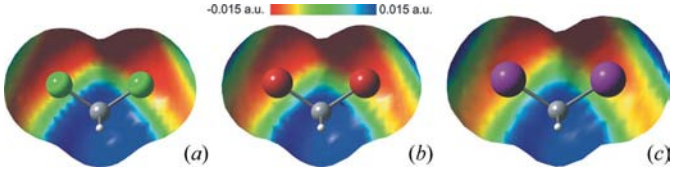

Figure 4
The molecular surfaces of (*a*) CH_2Cl_2, (*b*) CH_2Br_2 and (*c*) CH_2I_2 with their electrostatic potentials indicated in the colour scale. The colour scale range spans from −0.015 to 0.015 a.u.

The *a* parameter is most compressible and the shortest intermolecular halogen···halogen contacts, as seen in Fig. 3(*b*), form chains along [100].

3.3. Comparisons in dihalomethanes

3.3.1. Electrostatic potential calculations. The electrostatic potential calculations performed for CH_2X_2 (where X = Cl, Br, I) illustrate the differences in polarization in this series of molecules. The positive charge is located around the H atoms and at the 'cap' of the halogen atom at the extension of the C–halogen bond; the negative regions circumscribe the halogen atoms perpendicular to the C—X bond with the charge concentration between the halogen atoms (Fig. 4). The pressure-frozen structures of CH_2Br_2 and CH_2I_2 (Podsiadło *et al.*, 2006), and CH_2BrCl phase I are two-dimensionally isostructural (Fábián & Kálmán, 2004), and their similar charge distribution explains the head-to-tail arrangement of the molecules in columns. The electrostatic potential surface calculated for CH_2Cl_2, in comparison to CH_2Br_2 and CH_2I_2, has less positive atomic charges localized on the halogen atom along the C–halogen bond. This might explain the shift of CH_2Cl_2 molecules in a head-to-tail arrangement in columns.

The shortest halogen···halogen interactions observed in all the dihalomethane structures can be classified as type II (Pedireddi *et al.*, 1994; Price *et al.*, 1994; Ramasubbu *et al.*, 1986). These contacts are formed between the molecules in this manner; the shortest halogen···halogen contacts form an angle close to 180° with the C–halogen bond on one site (θ_1 angle) and an angle perpendicular to the C–halogen bond of the other molecule (θ_2 angle). The observed values of θ_1 for the pressure-frozen dichloro-, dibromo- and diiodomethane are: 168.72 (11), 179.3 (12) and 174.84 (3)°, respectively, while the θ_2 values in these compounds are: 118.31 (7), 112.7 (4) and 108.11 (2)°, respectively (Podsiadło *et al.*, 2005, 2006). In bromochloromethane phase II, θ_1 = 168.17 (5)° and θ_2 = 117.84 (2)°. The electrostatic potential surfaces explain this behaviour and show that the shortest halogen···halogen interactions in dihalomethane structures are mainly electrostatic in nature.

3.3.2. Thermodynamic properties. The known freezing pressures of dihalomethanes are inversely and approximately linearly correlated with the molecular weights (Fig. 5), irrespective of the crystal symmetries (Podsiadło *et al.*, 2005, 2006).

The shortest intermolecular halogen···halogen distances observed in all the pressure-frozen dihalomethane structures can also be correlated with the freezing pressure and molecular weight of these compounds (Fig. 6).

3.3.3. Compressibility of dihalomethanes. As shown in Fig. 7, the compressibility of dihalomethane compounds at 295 K is different and depends on halogen atoms. From ambient pressure to *ca* 0.1 GPa (freezing pressure of CH_2I_2), when all dihalomethane compounds are liquid, the compressibility correlates with the molecular weight, and decreases from CH_2Cl_2 to CH_2I_2. Up to *ca* 1.0 GPa, the limit imposed by the resistance of our cylinder-and-piston device, the compressibilities of CH_2Cl_2 and CH_2BrCl are remarkably similar. It is a

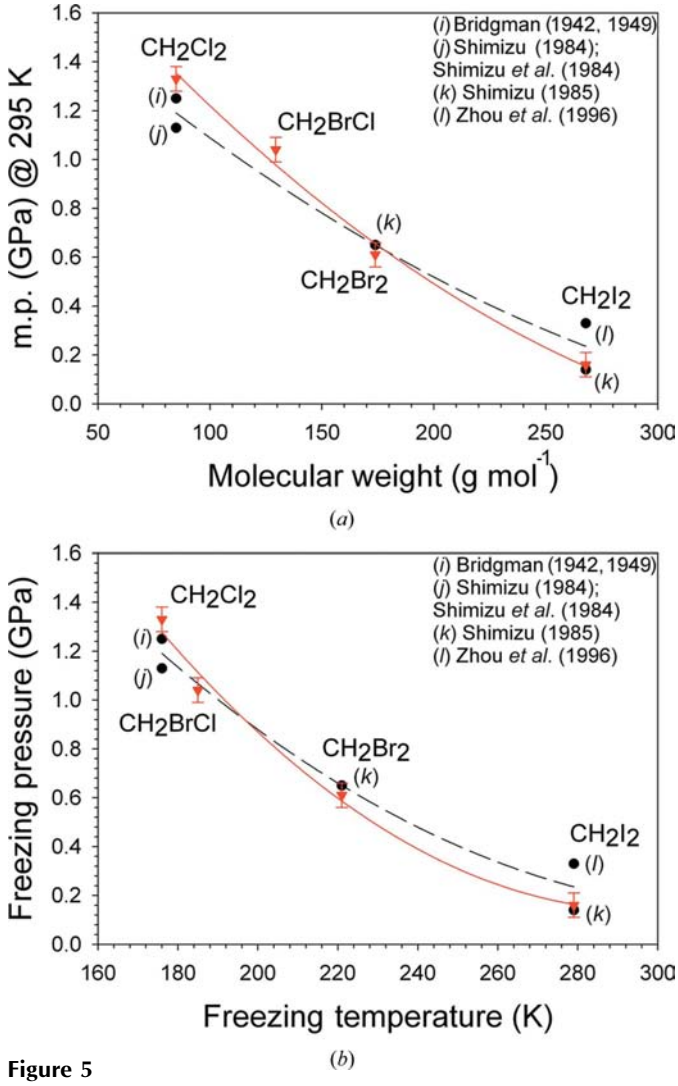

Figure 5
Freezing pressure of dihalomethanes as a function of (*a*) their molecular weight and (*b*) the freezing temperature. Full black circles joined by dashed lines represent the data measured by other research groups (see legends), while red triangles joined by full red lines represent the values measured in our laboratory for CH_2Cl_2, CH_2Br_2, CH_2I_2 (Podsiadło *et al.*, 2005, 2006) and CH_2BrCl.

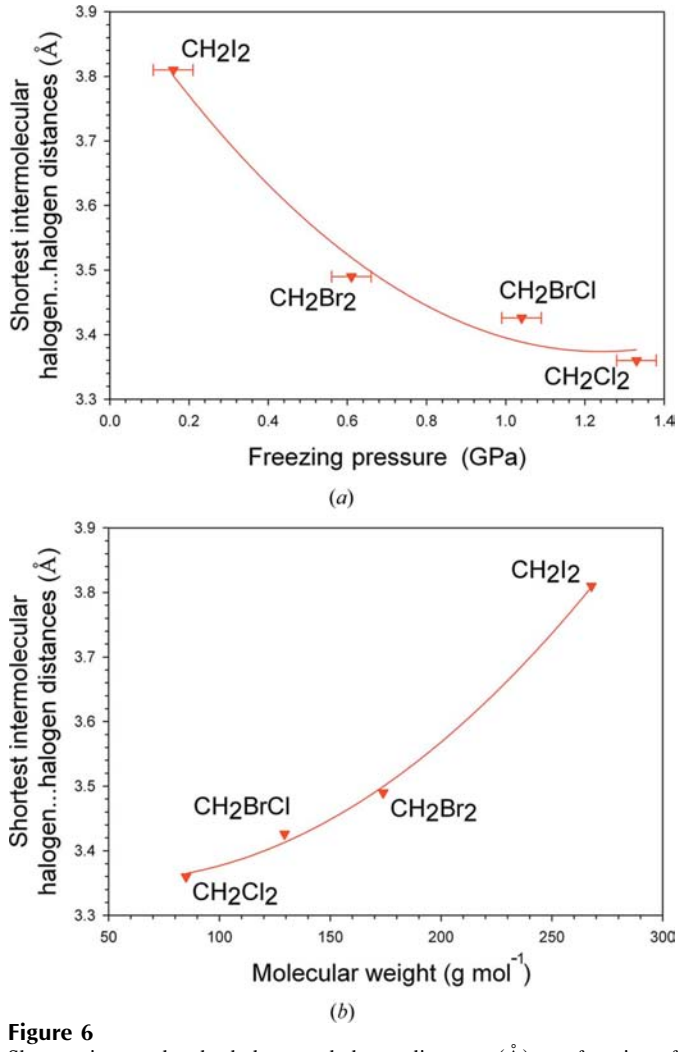

Figure 6
Shortest intermolecular halogen···halogen distances (Å) as a function of (*a*) freezing pressure and (*b*) molecular weight in a series of previously studied dihalomethanes (Podsiadło *et al.*, 2005, 2006) and in bromochloromethane phase II. The error bars, except the freezing-pressure values, are smaller than the symbols used.

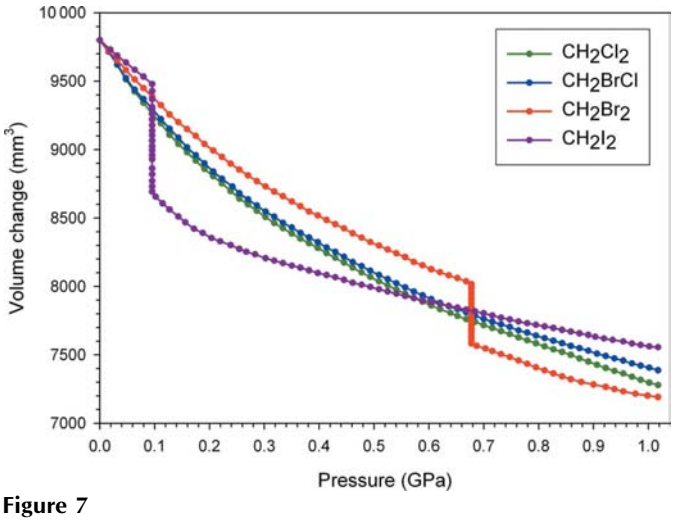

Figure 7
Compressibility of dihalomethanes from ambient pressure to *ca* 1 GPa at room temperature. Liquid–solid phase transitions are visible for CH_2Br_2 at *ca* 0.68 GPa (red dotted line) and CH_2I_2 at *ca* 0.1 GPa (violet line).

characteristic that the compression of liquid CH_2Br_2 and CH_2I_2 decreases at the pressures preceding their freezing, and that the isothermal freezing volume change ΔV_T make their compression larger than those of CH_2Cl_2 and CH_2BrCl. At still higher pressures the compression of solidified CH_2I_2 and CH_2Br_2 becomes smaller than the CH_2Cl_2 and CH_2BrCl liquids again. This characteristic 'take off' of the $V(p)$ curve for CH_2BrCl over the CH_2Cl_2 curve is observed between 0.8 and 1.0 GPa, although the crystallization of CH_2BrCl was not observed owing to the liquid superpressurizing effect. From the plots for CH_2I_2 and CH_2Br_2 it can be observed that ΔV_T decreases with pressure.

4. Conclusions

The isobaric and isochoric crystallization of CH_2BrCl illustrates the general properties of weak intermolecular interactions. The low-temperature freezing leads to the *C*2/*c* symmetric molecular arrangement governed by directional halogen···halogen and hydrogen···halogen intermolecular interactions. The charge distribution on the molecular surface shows that these intermolecular contacts are electrostatic in nature. In CH_2BrCl phase I the shortest halogen···halogen intermolecular interactions within the layers of molecules are electrostatically favourable, whereas between the layers short halogen···halogen intermolecular interactions are electrostatically unfavourable. Pressure favours the crystallization in phase II of CH_2BrCl, space group *Pbcn*, the close-packed structure of which is dominated by halogen···halogen interactions which are much shorter than in phase I.

This study was supported by the Polish Ministry of Scientific Research and Information Technology, Grant No. N N204 1956 33.

References

Awwadi, F. F., Willett, R. D., Peterson, K. A. & Twamley, B. (2006). *Chem. Eur. J.* **12**, 8952–8960.
Bader, R. F. W., Carroll, M. T., Cheeseman, J. R. & Chang, C. (1987). *J. Am. Chem. Soc.* **109**, 7968–7979.
Baranowski, B. & Moroz, A. (1982). *Polish J. Chem.* **56**, 379–391.
Barbour, L. J. (2001). *J. Supramol. Chem.* **1**, 189–191.
Barnett, J. D., Block, S. & Piermarini, G. J. (1973). *Rev. Sci. Instrum.* **44**, 1–9.
Batsanov, S. S. (2001). *Inorg. Mater.* **37**, 871–885.
Boese, R., Kirchner, M. T., Dunitz, J. D., Filippini, G. & Gavezzotti, A. (2001). *Helv. Chim. Acta*, **84**, 1561–1577.
Boldyreva, E. V. (2003). *Cryst. Eng.* **6**, 235–254.
Boldyreva, E. V., Ivashevskaya, S. N., Sowa, H., Ahsbahs, H. & Weber, H.-P. (2005). *Z. Kristallogr.* **220**, 50–57.
Boldyreva, E. V., Naumov, D. Yu. & Ahsbahs, H. (1998). *Acta Cryst.* B**54**, 798–808.
Bosch, E. & Barnes, C. L. (2002). *Cryst. Growth Des.* **4**, 299–302.
Bridgman, P. W. (1942). *J. Chem. Phys.* **9**, 794–797.
Bridgman, P. W. (1949). *Proc. Am. Acad. Arts Sci.* **77**, 129–146.
Budzianowski, A. & Katrusiak, A. (2004). *High-Pressure Crystallography*, edited by A. Katrusiak & P. F. McMillan, pp. 101–112. Dordrecht: Kluwer Academic Publishers.
Desiraju, G. R. & Parthasarathy, R. (1989). *J. Am. Chem. Soc.* **111**, 8725–8726.
Fábián, L. & Kálmán, A. (2004). *Acta Cryst.* B**60**, 547–558.
Frisch, M. J. *et al.* (2003). *GAUSSIAN*03, Revision B.04. Gaussian Inc., Pittsburgh, PA.
Grineva, O. V. & Zorkii, P. M. (2000). *Crystallogr. Rep.* **45**, 633–639.
Grineva, O. V. & Zorkii, P. M. (2001). *J. Struct. Chem.* **42**, 16–23.
Grineva, O. V. & Zorkii, P. M. (2002). *J. Struct. Chem.* **43**, 995–1005.
Grineva, O. V., Zorkii, P. M. & Rostov, E. S. (2007). *Struct. Chem.* **18**, 443–448.
Guru Row, T. N. & Parthasarathy, R. (1981). *J. Am. Chem. Soc.* **103**, 477–479.
Katrusiak, A. (2003). *REDSHABS.* Adam Mickiewicz University, Poznań, Poland.
Katrusiak, A. (2004). *Z. Kristallogr.* **219**, 461–467.
Kawaguchi, T., Tanaka, K., Takeuchi, T. & Watanabé, T. (1973). *Bull. Chem. Soc. Jpn*, **46**, 62–66.
Kawaguchi, T., Wakabayashi, A., Matsumoto, M., Takeuchi, T. & Watanabé, T. (1973). *Bull. Chem. Soc. Jpn*, **46**, 57–61.
Kitaigorodskii, A. I. (1973). *Molecular Crystals and Molecules.* New York: Academic Press.
Kitaigorodskii, A. I. (1983). *Smeshannye kristally*. Moscow: Izdatelstwo Nauka.
Metrangolo, P. & Resnati, G. (2001). *Chem. Eur. J.* **7**, 2511–2519.
Nyburg, S. C. & Faerman, C. H. (1985). *Acta Cryst.* B**41**, 274–279.
Oxford Diffraction (2004). *CrysAlis*, Version 1.171. Oxford Diffraction Ltd, Abingdon, Oxfordshire, England.
Pedireddi, V. R., Reddy, D. S., Goud, B. S., Craig, D. C., Rae, A. D. & Desiraju, G. R. (1994). *J. Chem. Soc. Perkin Trans. 2*, pp. 2353–2360.
Piermarini, G. J., Block, S., Barnett, J. D. & Forman, R. A. (1975). *J. Appl. Phys.* **46**, 2774–2780.
Podsiadło, M., Dziubek, K. & Katrusiak, A. (2005). *Acta Cryst.* B**61**, 595–600.
Podsiadło, M., Dziubek, K., Szafrański, M. & Katrusiak, A. (2006). *Acta Cryst.* B**62**, 1090–1098.
Price, S. L., Stone, A. J., Lucas, J., Rowland, R. S. & Thornley, A. E. (1994). *J. Am. Chem. Soc.* **116**, 4910–4918.
Prystupa, D. A., Torrie, B. H., Powell, B. M. & Gerlach, P. N. (1989). *Mol. Phys.* **68**, 835–851.
Ramasubbu, N., Parthasarathy, R. & Murray-Rust, P. (1986). *J. Am. Chem. Soc.* **108**, 4308–4314.

Rosenfield, R. E., Parthasarathy, R. & Dunitz, J. D. (1977). *J. Am. Chem. Soc.* **99**, 4860–4862.
Sheldrick, G. M. (1997*a*). *SHELXS*97. University of Göttingen, Germany.
Sheldrick, G. M. (1997*b*). *SHELXL*97. University of Göttingen, Germany.
Shimizu, H. (1984). *Chem. Phys. Lett.* **105**, 268–272.
Shimizu, H. (1985). *Solid State Physics under Pressure*, edited by S. Minomura, pp. 317–322. Tokyo: Terra Scientific Publishing Company.
Shimizu, H., Xu, J., Mao, H. K. & Bell, P. M. (1984). *Chem. Phys. Lett.* **105**, 273–276.
Weir, C. E., Piermarini, G. J. & Block, S. (1969). *J. Chem. Phys.* **50**, 2089–2093.
Zaman, B., Udachin, K. A. & Ripmeester, J. A. (2004). *Cryst. Growth Des.* **3**, 585–589.
Zhou, Y., Lee, S. A. & Anderson, A. (1996). *J. Raman Spectrosc.* **27**, 499–502.
Zordan, F. & Brammer, L. (2004). *Acta Cryst.* B**60**, 512–519.